25th IMEKO TC4 International Symposium
23rd International Workshop on ADC and DAC Modelling and Testing
IMEKO TC-4 2022
Brescia, Italy / September 12-14, 2022

Direct Comparison of Quantum Hall Resistance in Graphene and Gallium Arsenide in Liquid Helium

Ngoc Thanh Mai Tran[1,2], Jaesung Park[3], and Dong-Hun Chae[3*]

[1] *Politecnico di Torino, Corso Duca degli Abruzzi 24, 10129 Torino, Italy*
[2] *Istituto Nazionale di Ricerca Metrologica, Strada delle Cacce, 91, 10135 Torino, Italy*
[3]*Korea Research Institute of Standards and Science, Daejeon 34113, Republic of Korea*
N.T.M. Tran and J. Park contributed equally to this work.
[*]Corresponding author. e-mail:dhchae@kriss.re.kr

***Abstract* – Direct comparison of quantum Hall resistance in the same or different materials requires demanding experimental resources, such as two separate cryostats or a specially designed dual-socket probe operating far below the temperature of liquid helium. Here we experimentally demonstrate an efficient direct comparison of quantum Hall resistance in graphene and gallium arsenide/aluminium gallium arsenide heterostructure in liquid helium at 4.2 K with a standard probe from the practical point of view. To perform the direct comparison with one probe, we stacked two Hall devices with a printed circuit board and mating pins and employed a gallium arsenide Hall device with a high electron density. The direct comparison shows that the relative difference in quantized Hall resistance between the two materials in liquid helium is as small as 5 nΩ/Ω.**

I. INTRODUCTION

Precision comparisons of quantum Hall resistance such as the on-site comparison (BIPM.EM K-12) are of paramount importance in resistance metrology to verify the international coherence of primary resistance standards [1,2]. In such a comparison, two quantum Hall resistances (QHRs) in two separate cryostats are compared with each other via an artifact resistance reference. The transfer resistor exhibits instability with respect to temperature as well as intrinsic temporal drift. To avoid the relevant uncertainties, direct comparisons of QHRs in different materials have been performed below a temperature of 1 K for universality tests of QHRs, either in two separate cryostats [3-5] or in one cryostat hosting two Hall devices [6], since 1990. To simultaneously satisfy the quantization conditions of silicon metal–oxide–semiconductor field-effect transistor (Si-MOSFET) and gallium arsenide/ aluminium gallium arsenide (GaAs/AlGaAs) heterostructure Hall devices mounted in one probe under the same magnetic field, one of the two devices needs to be tilted with respect to the magnetic field direction [6], presenting an experimental challenge.

More recently, precise comparisons of the QHRs in graphene and GaAs/AlGaAs heterostructure have been accomplished either directly in two separate cryostats [4], or indirectly, in one cryostat with dual sockets via a resistance reference [7,8]. The required temperature is below 2 K to avoid dissipation in the quantum Hall state in GaAs/AlGaAs heterostructure, even though graphene exhibits good metrological quantization above 4.2 K [9], stemming from the linear energy-momentum dispersion [10,11] of massless Dirac fermions. To date, such a precision comparison has required demanding resources, such as two separate cryostats or a specially designed dual-socket probe operating below the temperature of liquid helium.

Here, we experimentally demonstrate a direct comparison of the QHRs in graphene and GaAs/AlGaAs heterostructure in liquid helium at 4.2 K with a standard probe. National metrology institutes commonly have a probe with a 12-pin transistor outline (TO-8) socket. We used such an ordinary probe to host two Hall devices. A graphene Hall device was mounted on a TO-8 chip carrier, made by printed circuit board (PCB) and mating pins. A GaAs/AlGaAs Hall device was stacked on top of the graphene Hall device with a PCB spacer. The pins of the TO-8 socket were shared by the two stacked Hall devices. To perform the direct comparison at 4.2 K, we employed a GaAs/AlGaAs Hall device with a high electron density whose quantization for a filling factor 2 is achieved above a magnetic field of 10 T [12]. The direct comparison of the QHRs in graphene and GaAs/AlGaAs heterostructure at 4.2 K showed that the relative difference between the two is smaller than 5 nΩ/Ω. We also showed that at 2.8 K, this relative difference is reduced to 2 nΩ/Ω, comparable to the expanded measurement uncertainty, due to dissipation reduction in the quantum Hall state in GaAs/AlGaAs heterostructure.

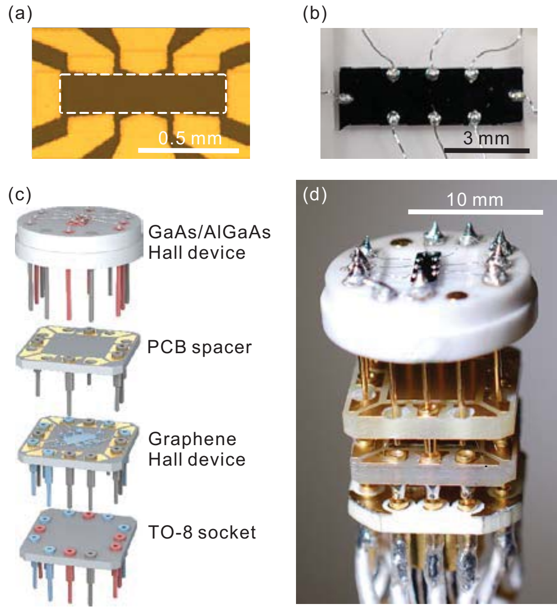

Fig. 1. Stacked Hall devices on the TO-8 socket. (a) Optical image of the graphene Hall device. The dashed line illustrates the boundary of the graphene channel. (b) Photograph of the GaAs/AlGaAs Hall device. (c) Schematic illustrations of the TO-8 socket, graphene Hall device, PCB spacer and GaAs/AlGaAs Hall device. The pins of the TO-8 socket were shared by the graphene and GaAs/AlGaAs Hall devices through stacking, as shown by color coding in blue and red, respectively. (d) Photograph of the two stacked Hall devices mounted on the TO-8 socket.

II. DEVICE AND EXPERIMENTAL SETUP

The graphene Hall device was fabricated with epitaxial graphene grown on silicon carbide (SiC). For graphene synthesis on SiC, the SiC substrate was heated to 1600 °C in a hot-wall reactor to sublimate the Si atoms [13]. High-quality graphene with a low step height, typically below 1 nm, and large monolayer coverage is essential for the realization of a graphene-based quantum Hall resistance standard. We used a modified graphite susceptor with a small gap [14] and the polymer-assisted growth technique [15] to prevent step bunching, resulting in a smooth graphene morphology on the SiC. Electron-beam lithography for the patterning of the graphene channel and electron-beam evaporation for the metal contact were applied to fabricate the graphene device. Polymer-assisted hole-doping of the graphene was adopted to fulfill the quantization condition of a filling factor 2 at a lower magnetic field [16]. We also employed a GaAs/AlGaAs Hall device (PTB 130-20) with a high electron density, fabricated by the Physikalisch-Technische Bundesanstalt (PTB), for operation at liquid helium temperature [12]. The carrier type, density and mobility of the graphene device were hole, 2.3×10^{11} cm^{-2} and

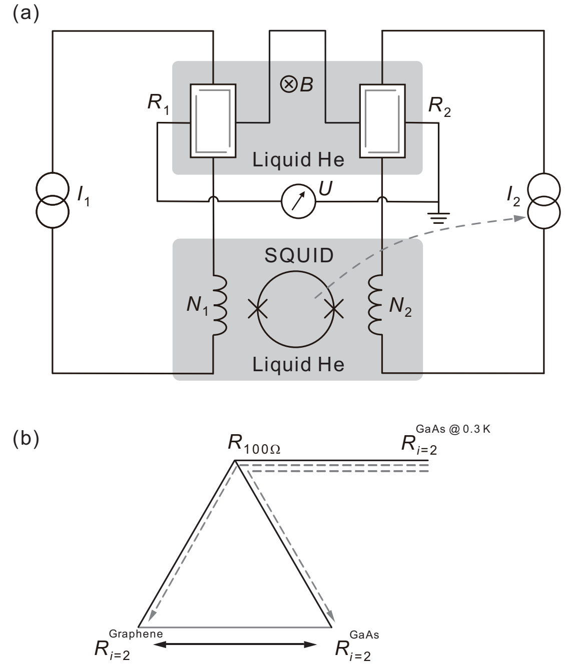

Fig. 2. Schematic of the direct comparison of the QHRs in the graphene and GaAs/AlGaAs Hall devices. (a) Circuit diagram of the cryogenic current comparator bridge for direct comparison. (b) The solid arrow represents the direct comparison between the QHRs realized in the graphene and GaAs/AlGaAs Hall devices. The dashed lines represent traceable measurements via a 100 Ω resistance reference with respect to a QHR standard operating at 0.3 K.

5 290 cm^2 V^{-1} s^{-1}, respectively. The carrier type, density and mobility of the GaAs/AlGaAs Hall device were electron, 5.3×10^{11} cm^{-2} and 585 000 cm^2 V^{-1} s^{-1}, respectively. These parameters were evaluated via magnetoresistance measurements in the classical Hall regime. Figure 1(a) and (b) show images of the graphene and GaAs/AlGaAs Hall devices, respectively. The contact resistance was determined in three terminal configuration [17] at the quantum Hall state. The contact resistances of graphene and GaAs devices were approximately 1 Ω and 2 Ω, respectively.

For direct comparison of the QHRs in graphene and GaAs/AlGaAs heterostructure, the graphene and GaAs/AlGaAs Hall devices are loaded into an ordinary probe with a 12-pin TO-8 socket. The GaAs/AlGaAs Hall device was stacked on top of the graphene device, as depicted in Fig. 1(c) and (d). The graphene Hall device was mounted on the TO-8 PCB carrier using 6 selected pins, color coded in blue in Fig. 1(c). The other 5 pins of the TO-8 socket, color coded in red, were connected to the 5 leads of the GaAs Hall device. A PCB adaptor with only 5 mating pins and 7 through-holes, as illustrated in Fig. 1(c), was stacked on the graphene TO-8 carrier. The standard GaAs/AlGaAs Hall device was finally plugged into the PCB adaptor, with only 5 pins electrically connected to the

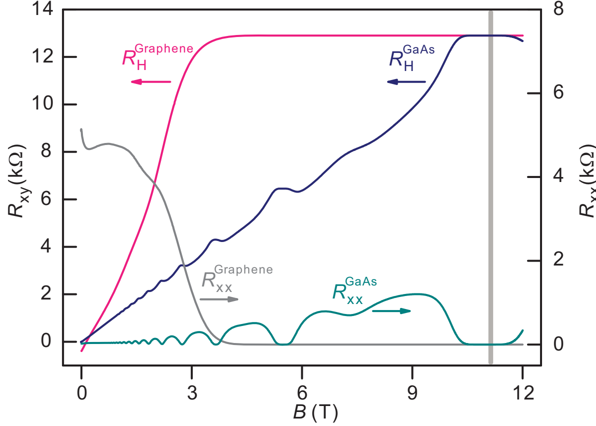

Fig. 3. Magnetoresistance measurements of the graphene and GaAs/AlGaAs Hall devices immersed in liquid helium at 4.2 K. The Hall and longitudinal resistances of the graphene (GaAs/AlGaAs) device are represented by the red (blue) and gray (teal-gray) traces, respectively. The center of the quantized Hall resistance plateau for a filling factor 2 in GaAs/AlGaAs corresponds to a magnetic field of 11 T. The left and right vertical axes display the Hall and longitudinal resistances, respectively.

red-colored pins in the TO-8 socket. The pins of the TO-8 socket were accordingly shared by the two Hall devices through this stacking method.

We employed a helium bath cryostat with a 12 T superconducting magnet. Most of the experiments were performed at 4.2 K. If necessary, the liquid helium temperature can be lowered with a λ-point refrigerator with which the superconducting magnet is equipped. Direct comparison of the QHRs in the graphene and GaAs/AlGaAs Hall devices was performed with a cryogenic current comparator (CCC) bridge [18]. The two Hall devices were loaded in a standard probe with one TO-8 socket immersed in liquid helium. The schematic bridge circuit is shown in Fig. 2(a). The direct comparison was confirmed by an indirect comparison based on conventional traceable resistance measurements via a transfer resistor [18], as illustrated by dashed lines in Fig. 2(b).

III. EXPERIMENTAL RESULTS

A. Magnetoresistance Measurements of the Graphene and GaAs/AlGaAs Hall Devices

Figure 3 shows the Hall resistances and the longitudinal resistances of the graphene and GaAs/AlGaAs Hall devices as functions of the magnetic field in liquid helium at 4.2 K. The Hall resistance ($R_H^{Graphene}$) of the graphene starts to be quantized above a magnetic field of approximately 4 T. The wide Hall plateau for a filling factor 2 (i = 2) in epitaxial graphene, stemming from the magnetic-field-dependent charge transfer between the SiC and graphene [19], is distinct from that of exfoliated

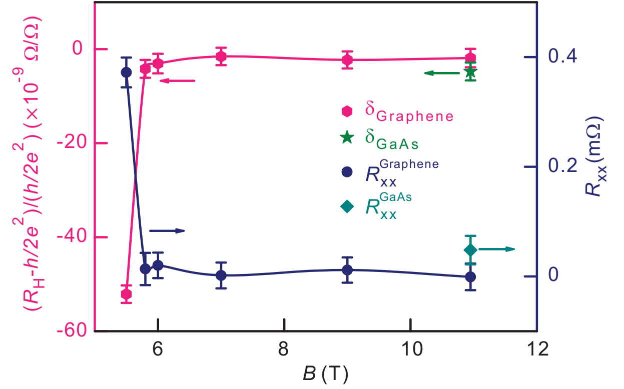

Fig. 4. Relative deviation of the Hall resistance from $\frac{h}{2e^2}$ and the longitudinal resistance measured at 4.2 K. The measurements of the relative deviation and longitudinal resistance in the graphene device are plotted as red hexagons and blue circles, respectively. The green star and teal-gray diamond depict the relative deviation and longitudinal resistance, respectively, of the GaAs/AlGaAs device at 11 T. Error bars of R_{xx} and relative deviation indicate the expanded measurement uncertainty (k=2).

graphene. The corresponding longitudinal resistance ($R_{xx}^{Graphene}$) for i = 2 is suppressed above 4 T. The measured Hall (R_H^{GaAs}) and longitudinal (R_{xx}^{GaAs}) resistances of the GaAs/AlGaAs device overlap with the magnetoresistance traces of the graphene device. The center of the quantized Hall plateau at i = 2 corresponds to a magnetic field of 11 T. The precise direct comparison of the two QHRs was performed at this magnetic field. We note that the common quantization condition for the graphene and GaAs/AlGaAs heterostructure under the same magnetic field can be easily satisfied thanks to the wide quantized Hall resistance plateau of epitaxial graphene, unlike in the direct comparison of Si-MOSFET and GaAs/AlGaAs heterostructure [6].

B. Traceable Measurements of the QHRs in Graphene and GaAs/AlGaAs heterostructure

Prior to the direct comparison, precision measurements of the QHRs in the graphene and GaAs/AlGaAs heterostructure were performed with the CCC bridge by comparing the QHR against a 100 Ω resistance reference, which was precalibrated with respect to a QHR standard realized in GaAs/AlGaAs heterostructure operating at 0.3 K [18]. For these conventional traceable measurements, an auxiliary winding and current source were included in the bridge circuit [18, 20], although this is not shown in Fig. 2(a). The longitudinal resistance was also measured with the CCC bridge. The difference between the ordinary Hall resistance and a Hall resistance measured with a diagonal contact pair corresponds to the longitudinal resistance [21].

Figure 4 shows the relative deviation of the measured Hall resistance from the nominal QHR ($\frac{h}{2e^2}$) at i = 2 with

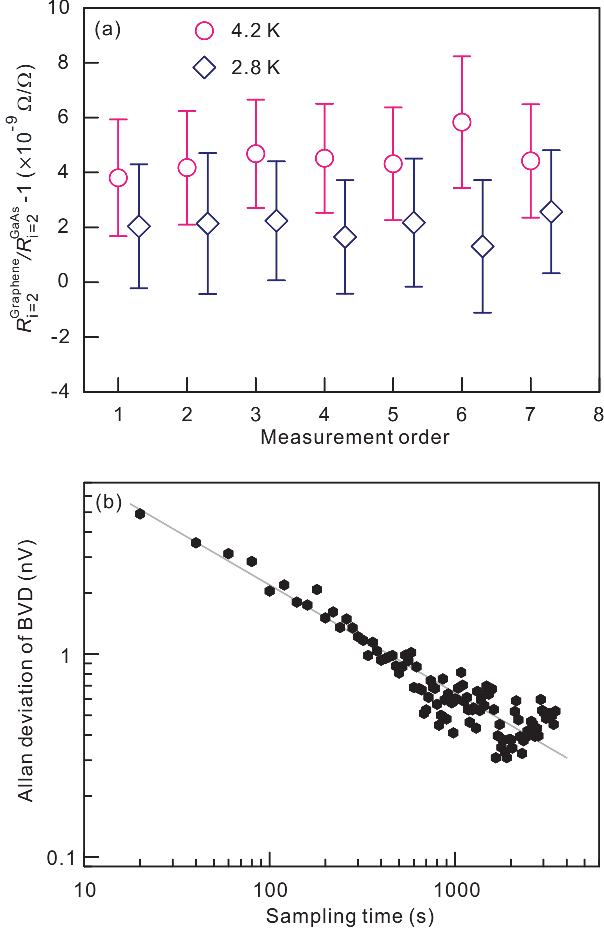

Fig. 5. Direct comparison of the QHRs in the graphene and GaAs/AlGaAs heterostructure and the Allan deviation of the bridge voltage difference. (a) Repeated measurements of the relative difference between the QHRs in the graphene and GaAs/AlGaAs Hall devices in liquid helium under a magnetic field of 11 T at 4.2 K and 2.8 K, represented by circular and diamond symbols, respectively. (b) Allan deviation of the bridge voltage difference for direct comparison from a data set acquired for 4 hours at 4.2 K. The inverse square root time dependence $(1/\sqrt{\tau})$ *of white noise overlaps with the Allan deviation plot.*

respect to the magnetic field at 4.2 K. The longitudinal resistance is also depicted. The red hexagons and blue circles represent the measurements of the relative deviation and longitudinal resistance, respectively, in the graphene Hall device. The quantized Hall resistance starts to deviate from the nominal value below a magnetic field of 6 T. The Hall resistances in the plateau are equivalent to $\frac{h}{2e^2}$ within the measurement uncertainty. The longitudinal resistance accordingly becomes larger than the measurement uncertainty of 23 μΩ below 6 T. The deviation and longitudinal resistance acquired at the central value (11 T) of the filling factor 2 Hall plateau in the GaAs/AlGaAs Hall device are depicted by star and diamond symbols, respectively. The finite relative deviation of approximately 4.8 nΩ/Ω from the nominal quantized resistance and the finite longitudinal resistance of 48 μΩ are observed at the plateau center. A ratio of the relative deviation to the longitudinal resistance is defined as the *s*-parameter [21]. The *s*-parameter can be also evaluated using a dip at the edge of the Hall plateau and the corresponding longitudinal resistance. It turns out that the *s*-parameter is approximately -0.8. The estimated *s*-parameters with the above two methods are comparable. It implies that the deviation is attributed to a dissipation in the quantum Hall state at the given temperature, which will be discussed in detail later.

C. Direct Comparison of the QHRs in Graphene and GaAs/AlGaAs heterostructure in Liquid Helium

The direct comparison of the QHRs in the graphene and GaAs/AlGaAs Hall devices in liquid helium was performed with the CCC bridge as illustrated in Fig. 2(a). A magnetic field of 11 T was applied because this value lies at the center of the quantized Hall resistance plateau at $i = 2$ for the GaAs/AlGaAs Hall device and simultaneously lies within the wide Hall resistance plateau at $i = 2$ for the epitaxial graphene device.

The circular symbols in Fig. 5(a) represent repeated measurements of the relative difference in the QHRs of the graphene and GaAs/AlGaAs devices in liquid helium at 4.2 K. The acquisition time for each measurement was approximately 16 minutes. The mean relative difference from 7 data sets is approximately 4.5 nΩ/Ω. From the traceable measurements of the QHRs in the graphene and GaAs/AlGaAs heterostructure, as illustrated in Fig. 2(b) and Fig. 4, the relative difference was indirectly determined via the 100 Ω resistance reference, yielding a value of approximately 3.5 nΩ/Ω, consistent with that found in the direct comparison within the measurement uncertainty.

To identify the origin of the finite relative difference at 4.2 K, as plotted in Fig. 5, we also performed a direct comparison at a lower temperature. As shown in Fig. 4, the Hall resistance of the GaAs/AlGaAs heterostructure deviates from the nominal resistance at $i = 2$, and there exists a corresponding longitudinal resistance larger than the measurement uncertainty. These observations indicate that the dissipation in the GaAs/AlGaAs heterostructure at this temperature may lead to a Hall resistance deviation and a finite longitudinal voltage drop. The diamond symbols in Fig. 5 represent the relative differences measured at a lower temperature of 2.8 K, which was achieved by means of the λ-point refrigerator at the superconducting magnet. This experiment clearly shows that the relative difference is reduced to 2 nΩ/Ω at this temperature. This indicates that the relative difference can be attributed to dissipation in the quantum Hall state in the GaAs/AlGaAs heterostructure, which is inefficiently cooled at the given temperatures. Nevertheless, the direct

Table 1. Uncertainty budge for a typical measurement of the resistance ratio via direct comparison

Contribution	Uncertainty (nΩ/Ω)
Winding ratio error	0.6
Insulation	0.4
SQUID resolution	0.1
Miscellaneous	<0.1
ΔU (type A)	0.5
Expanded measurement uncertainty (k = 2)	1.7

comparison in liquid helium at 4.2 K shows that the relative difference in the QHR in the graphene and GaAs is smaller than 5 nΩ/Ω. Note that this stacking method can be employed to compare QHRs in GaAs/AlGaAs heterostructure and other materials, including graphene, for universality tests in an ultimate precision with an existing metrological probe at lower temperatures.

We performed a long direct comparison measurement to investigate the Allan deviation in the setup. Figure 5 (b) shows the Allan deviation of the bridge voltage difference from a data set acquired for 4 hours at 4.2 K. The Allan deviation follows an inverse square root time dependence $(1/\sqrt{\tau})$ up to a sampling time of a few thousand seconds. This indicates that uncorrelated white noise is predominant in the direct comparison measurement. Additionally, the statistical measurement uncertainty can be reduced to a few parts in 10^{10} for the employed acquisition time scale. Note that error bar indicates the expanded measurement uncertainty (k=2).

D. Uncertainty Budget for Direct Comparison

Table I summarizes the contributions to the uncertainty budget for a typical measurement of the resistance ratio via the direct comparison. The overall expanded measurement uncertainty (k = 2) at the 95% confidence level is typically smaller than 2 nΩ/Ω. A significant contribution comes from the winding ratio error. Although the winding ratio error test showed an uncertainty of approximately a few nΩ/Ω, we conservatively assume an error of one part in 10^9. This leads to a value of 0.6 nΩ/Ω when the rectangular distribution is taken into account. The electric insulation of 20 TΩ results in an uncertainty of approximately 0.4 nΩ/Ω. We note that the electrical insulation resistance was measured between a lead and an outer chassis of probe shorted to ground with all the other leads shorted to the chassis. The flux resolution limit of the employed SQUID also contributes to the uncertainty. The flux via the 2048-turn coil induced by a driving current of 38.74 μA is determined by the flux linkage [23] of 11 $\mu\text{A}\cdot\text{turns}/\phi_o$ to be approximately $7200\phi_o$. Here, ϕ_o is the quantum of the flux $(h/2e)$. There is some evidence from ratio error tests on CCCs that rectification of noise can cause flux errors at the level of $1\ \mu\phi_o$ in SQUIDs similar to the one used in this study [24]. We therefore assign an uncertainty of $1\ \mu\phi_o$ to the SQUID output, and the corresponding flux error becomes $1\mu\phi_o/7200\phi_o$. When the rectangular distribution is considered, the relative uncertainty becomes close to 0.1 nΩ/Ω. Other minor uncertainties include the voltage measurement error of the nanovoltmeter in the bridge, which is smaller than 0.1 nΩ/Ω. The statistical type-A uncertainty of the bridge voltage difference is typically close to 0.5 nΩ/Ω for the employed data acquisition time.

IV. SUMMARY

In summary, we have demonstrated a direct comparison of quantized Hall resistance at a filling factor 2 in graphene and GaAs/AlGaAs heterostructure by a single standard metrological probe at the liquid helium temperature of 4.2 K with less demanding resources from the practical point of view. For this direct comparison, we employed a gallium arsenide Hall device with a high electron density stacked on top of a graphene Hall device with a printed circuit board adaptor to share the limited pins of a standard socket. This direct comparison shows that the difference between the quantum Hall resistances in graphene and GaAs/AlGaAs heterostructure in liquid helium is as small as 5 nΩ/Ω. This difference, which is reduced at the lower temperature, is attributed to the dissipation of the quantum Hall state in gallium arsenide in liquid helium. We note that this paper is about the impementation of the comparison method with a single conventional probe, not about the result itself of the comparison.

ACKNOWLEDGMENT

This research was supported by the Research on the Redefinition of SI Base Units project (Grant No. KRISS-2022-GP2022-0001) funded by the Korea Research Institute of Standards and Science. This work was supported in part by the Joint Research Project GIQS (18SIB07). This project also received funding from the European Metrology Programme for Innovation and Research (EMPIR) co-financed by the Participating States and from the European Union's Horizon 2020 research and innovation programme. In Korea, this collaborative work was supported by the National Research Foundation of Korea (Grant No. NRF-2019K1A3A1A78077479).

REFERENCES

[1] F. Delahaye and D. Dominguez, "Precise comparisons of quantized Hall resistances," in *IEEE Trans. Instrum. Meas.*, vol. IM-36, no. 2, pp. 226-229, Jun. 1987.

[2] F. Delahaye, T. J. Witt, F. Piquemal, and G. Geneves, "Comparison of quantum Hall effect resistance standards of the BNM/LCIE and the BIPM," in *IEEE Trans. Instrum. Meas.*, vol. 44, no. 2, pp. 258-261, Apr. 1995-

[3] B. Jeckelmann, B. Jeanneret, and D. Inglis, “High-precision measurements of the quantized Hall resistance: Experimental conditions for universality,” in *Phys. Rev. B*, vol. 55, iss. 19 – 15, May 1997.

[4] T. J. B. M. Janssen, *et al.*, “Precision comparison of the quantum Hall effect in graphene and gallium arsenide,” in *Metrologia,* vol. 49, pp. 294, Feb. 2012.

[5] F. J. Ahlers, M. Götz, and K. Pierz, “Direct comparison of fractional and integer quantized Hall resistance,” in *Metrologia*, vol. 54, pp. 516, Jun. 2017.

[6] A. Hartland, *et al.*, “Direct comparison of the quantized Hall resistance in gallium arsenide and silicon,” in *Phys. Rev. Lett*., vol. 66, pp. 969, Feb. 1991.

[7] D. G. Jarrett *et al.,* "Transport of NIST Graphene Quantized Hall Devices and Comparison with AIST Gallium-Arsenide Quantized Hall Devices," in *2018 Conference on Precision Electromagnetic Measurements (CPEM 2018),* Paris, 2018, pp. 1-2.

[8] S. U. Payagala *et al.,* "Comparison Between Graphene and GaAs Quantized Hall Devices With a Dual Probe," in *IEEE Trans. Instrum. Meas.,* vol. 69, no. 12, pp. 9374-9380, Dec. 2020.

[9] R. Ribeiro-Palau, F. Lafont, J. Brun-Picard, *et al*., “Quantum Hall resistance standard in graphene devices under relaxed experimental conditions,” in *Nat. Nanotechnol,* vol. 10, pp. 965–971, Nov. 2015.

[10] K. Novoselov, A. Geim, S. Morozov *et al*., “Two-dimensional gas of massless Dirac fermions in graphene,” in *Nature,* vol. 438, pp. 197–200 Sep. 2005.

[11] Y. Zhang, Y-W. Tan, H. Stormer, *et al.,* “Experimental observation of the quantum Hall effect and Berry's phase in graphene,” in *Nature,* vol. 438, pp. 201–204, Sep. 2005.

[12] J. Kučera, P. Svoboda, and K. Pierz, "AC and DC Quantum Hall Measurements in GaAs-Based Devices at Temperatures Up To 4.2 K," in *IEEE Trans. Instrum. Meas.,* vol. 68, no. 6, pp. 2106-2112, Jun. 2019.

[13] M. Ostler, F. Speck, M. Gick, and T. Seyller, “Automated preparation of high-quality epitaxial graphene on 6H-SiC(0001),” in *Phys. Status Solidi B,* vol. 247, pp. 2924 – 2926, Dec. 2010.

[14] J. Park, W.-S. Kim, and D.-H. Chae, “Realization of $5h/e^2$ with graphene quantum Hall resistance array”, in *Appl. Phys. Lett*. vol. 116, 093102, Mar. 2020.

[15] M. Kruskopf, M. D. Pakdehi, K. Pierz, S. Wundrack, R. Stosch, T. Dziomba, M. Götz, J. Baringhaus, J. Aprojanz, C. Tegenkamp, J. Lidzba, T. Seyller, F. Hohls, F. J. Ahlers, and H. W. Schumacher, “Comeback of epitaxial graphene for electronics: large-area growth of bilayer-free graphene on SiC,” in *2D Materials,* vol. 3, 041002, Jun. 2016.

[16] H. He, K.H. Kim, A. Danilov, *et al*., “Uniform doping of graphene close to the Dirac point by polymer-assisted assembly of molecular dopants,” in *Nat Commun*, vol. 9, 3956, Sep. 2018.

[17] G. L. J. A. Rikken, *et al.*, “Two-terminal resistance of quantum Hall devices” in *Phy. Rev. B* vol. 37, 6181, Apr. 1988.

[18] P. Gournay, B. Rolland, D.-H. Chae and W.-S. Kim, “On-site comparison of quantum Hall effect resistance standards of the KRISS and the BIPM: ongoing key comparison BIPM.EM-K12,” in *Metrologia Tech. Suppl*., vol. 57, 01010, 2020.

[19] T. J. B. M. Janssen, *et al.*, “Anomalously strong pinning of the filling factor $\nu=2$ in epitaxial graphene,” in *Phys. Rev. B*, vol. 83, 233402, Jun. 2011.

[20] D.-H. Chae, W-S. Kim, T. Oe and N.-H. Kaneko, “Direct comparison of 1 MΩ quantized Hall array resistance and quantum Hall resistance standard”, in *Metrologia*, vol. 55, 645, Jul. 2018.

[21] F. Delahaye and B. Jeckelmann B, “Revised technical guidelines for reliable dc measurements of the quantized Hall resistance”, in *Metrologia*, vol. 40, 217, Sep. 2003.

[22] D. Drung and J. Storm, “Ultralow-noise chopper amplifier with low input charge injection”, in *IEEE Trans. Instrum. Meas*, vol. 60, no. 7, pp. 2347-2352, Jul. 2011.

[23] D. Drung, *et al.*, “Improving the stability of cryogenic current comparator setups”, in *Supercond. Sci. Technol.*, vol. 22, no. 11, 114004, Oct. 2009.

[24] D. Drung, M. Götz, E. Pesel, and H. Scherer, "Improving the Traceable Measurement and Generation of Small Direct Currents," in *IEEE Trans. Instrum. Meas*., vol. 64, no. 11, pp. 3021-3030, Nov. 2015.